J. Fluid Mech. (1981), *vol.* 104, *pp.* 217–246
Printed in Great Britain

The coupling between flow instabilities and incident disturbances at a leading edge

By M. E. GOLDSTEIN

National Aeronautics and Space Administration, Lewis Research Center, Cleveland, Ohio 44135

(Received 28 January 1980)

It is now generally agreed that an external disturbance field, such as an incident acoustic wave, can effectively couple to instabilities of a flow past a trailing edge. One purpose of the present paper is to show that there are situations where a similar coupling can occur at a leading edge. The process is analysed and the effects of experimentally controllable parameters are assessed. It is important to account for such phenomena when evaluating the effect of external disturbances on transition.

1. Introduction

The effects of viscosity cannot always be ignored when calculating the steady or unsteady flows about solid obstacles even when the Reynolds numbers are large. But when the obstacle is thin in one of its transverse dimensions (relative to its streamwise dimension) and the amplitude of the unsteady velocity is small relative to the mean flow velocity (or relative to the velocity of sound if the frequency is high enough) the dominant viscous effects will often act along one or more lines such as the trailing edge of the obstacle. In which case it is usually possible to incorporate the viscous effects into an otherwise inviscid solution to the problem by imposing a 'Kutta' condition – which requires that the solution remain finite at the trailing edge.

When there is no mean flow and the edge of a flat plate is subjected to a small-amplitude unsteady motion (say an incident acoustic field) the correct inviscid solution will exhibit a square-root singularity at that edge. But when a mean flow is imposed on one or both sides of the plate the singularity at a trailing edge will be smoothed out by a continuous shedding of vorticity that is convected downstream by the mean flow. This vortex shedding can generally be incorporated into an inviscid model of the flow, but the amount of shed vorticity must then be determined by consideration of viscous effects. It turns out that this quantity is directly related to the level of the trailing edge singularity. The 'Kutta' condition requires that the amount of shed vorticity be just sufficient to eliminate the singularity at the trailing edge. This leads to a uniquely specified boundary value problem for the inviscid flow equations.

Calculations involving viscosity (Brown & Daniels 1975; Daniels 1978; Rienstra 1979) confirm the validity of the 'Kutta' condition for sufficiently high Reynolds number laminar flows whose frequencies and unsteady amplitudes are sufficiently small. There are also a number of carefully controlled experiments (Bratt 1953; Ohashi & Ishikawa 1972; Kovasznay & Fujita 1973; Heavens 1978; Bechert & Pfizen-

0022-1120/81/4725-3460 $02.00

maier 1975) which generally indicate that the 'Kutta' condition will be satisfied whenever the amplitude and frequency of the unsteady motion are not too large.

The vortex shedding can frequently be accounted for by allowing a thin vortex sheet to extend downstream from the trailing edge whenever the mean flow velocity is substantially the same on both sides of this edge, as it would be, say, for an airfoil. The vorticity in this sheet is convected downstream with unchanged amplitude at the velocity of the mean flow. Since Wagner's (1925) original study of the lift on impulsively started airfoils, most analyses of the unsteady airfoil problem have accounted for this effect. The strength of the vortex sheet is usually determined by requiring that the 'Kutta' condition be satisfied.

The case where there is a finite mean flow on one side of the obstacle and zero mean flow on the other has been considered only recently. This configuration is fairly representative of the flow near a nozzle lip. Crighton & Leppington (1974) considered the unsteady flow produced by a time-harmonic acoustic source near the edge of a semi-infinite flat plate which has a uniform mean flow on one side and zero mean flow on the other and extends to infinity in the upstream direction. They showed that this problem does not possess a solution that remains finite at all points of space. Its solution will either exhibit a singularity at the trailing edge or will grow exponentially fast at downstream infinity, or both. Mathematically, this case differs from the one where the mean flow is the same on both sides of the plate because the latter problem possesses an eigensolution that (1) has a tangential velocity discontinuity across a sheet which extends downstream from the trailing edge, that (2) remains bounded at infinity, and that (3) has a square root singularity at the edge. Then since it is permissible to add an arbitrary multiple of this eigensolution to the particular solution which is continuous everywhere downstream of the trailing edge and since this latter solution also possesses a square root singularity at the edge, the arbitrary constant can always be adjusted to cancel out the singularity between these two solutions.

When the mean velocity is discontinuous across the plate, the eigensolution corresponds to a spatially growing Helmholtz instability of the velocity discontinuity shear layer and must therefore grow exponentially with downstream distance (Crighton & Leppington 1974; Rienstra 1979). The solution to the problem will then be exponentially large at infinity if this eigensolution is added in to cancel the square root singularity at the trailing edge. But, such behaviour is not necessarily inconsistent with the physics of the problem since the linear solution is only expected to be valid in a local region near the edge. Then, since the instability wave becomes excessively large only when it is outside of this region, there is some hope that its large magnitude will not substantially alter the local solution near the edge.

In any case, this triggering of the instability by an incident acoustic signal now appears to be well verified experimentally (Bechert & Pfizenmaier 1975) and, in many instances, the 'Kutta' condition actually seems to be satisfied.

When the time-harmonic solution is not required to be bounded at infinity some additional condition must be imposed in order to make it unique. We have seen that this can sometimes be accomplished by imposing a 'Kutta' condition at a trailing edge. However, it can also be accomplished by finding the long time behaviour of the solution to the corresponding initial-value problem that has minimum edge singularity and satisfies causality in the sense that the flow is identically zero before

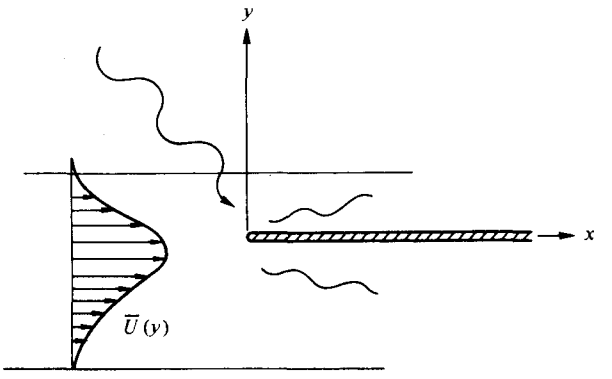

FIGURE 1. Orientation of plate in sheared mean flow.

the incident disturbance is 'switched on'. These two conditions lead to the *same solution* for the trailing-edge problem of Crighton & Leppington (1974)!

Now Crighton & Leppington did not stress the 'Kutta' condition but rather emphasized causality as being crucial for their result. Rienstra (1979), on the other hand, argues that causality is irrelevant in periodic flows that exist for all time and that the appropriate boundary condition is then an edge condition, such as 'Kutta' condition, which is determined solely by viscous and nonlinear effects. He points out that the memory of the real physical system cannot, in reality, be very long, with the variety of random disturbances that must always occur, and that the transient response field which cannot match the edge condition must be swept away by the flow. But mathematically the causality condition acts as a sort of '*radiation condition for instability waves*', which ensures that all such disturbances travel outward from their source, and, unlike the causality condition, the 'Kutta' condition is not always sufficient to determine the solution even for some trailing-edge problems uniquely.

Thus it is possible that singularities in the inviscid solution are often eliminated or at least minimized by the triggering of a spatially growing instability wave in the downstream region and that the flow separation that might otherwise occur is thereby prevented or perhaps moderated. Now the unsteady inviscid flow solutions also become singular at sharp *leading* edges. But it frequently happens that this singularity cannot be eliminated by a downstream instability because the latter's growth is inhibited in the narrow and highly stable boundary layer that usually occurs near the leading edge. The singularity must then be relieved by viscous and nonlinear effects and it might ultimately lead to unsteady flow separation.† But it is quite easy to induce an instability wave downstream of a leading edge when it is embedded in an inflexional shear flow in the manner indicated in figure 1 – especially when this flow is on the verge of becoming unstable. Such spatially growing instability waves are clearly shown in figure 2, which is comprised of photographs of the flow over a wedge placed in a rectangular laminar jet. (The flow here is from left to right.) The photographs were taken during an edge tone experiment and the unsteady motion that triggered the instability wave could have been an acoustic wave reflected from the nozzle lip or a harmonic disturbance convected downstream by the mean flow, or perhaps both. We shall not attempt to analyse this rather complicated flow. But suppose that an unsteady disturbance is incident on the leading edge of a long

† A true singularity will only exist if the edge is infinitely sharp: this is never the case in practice.

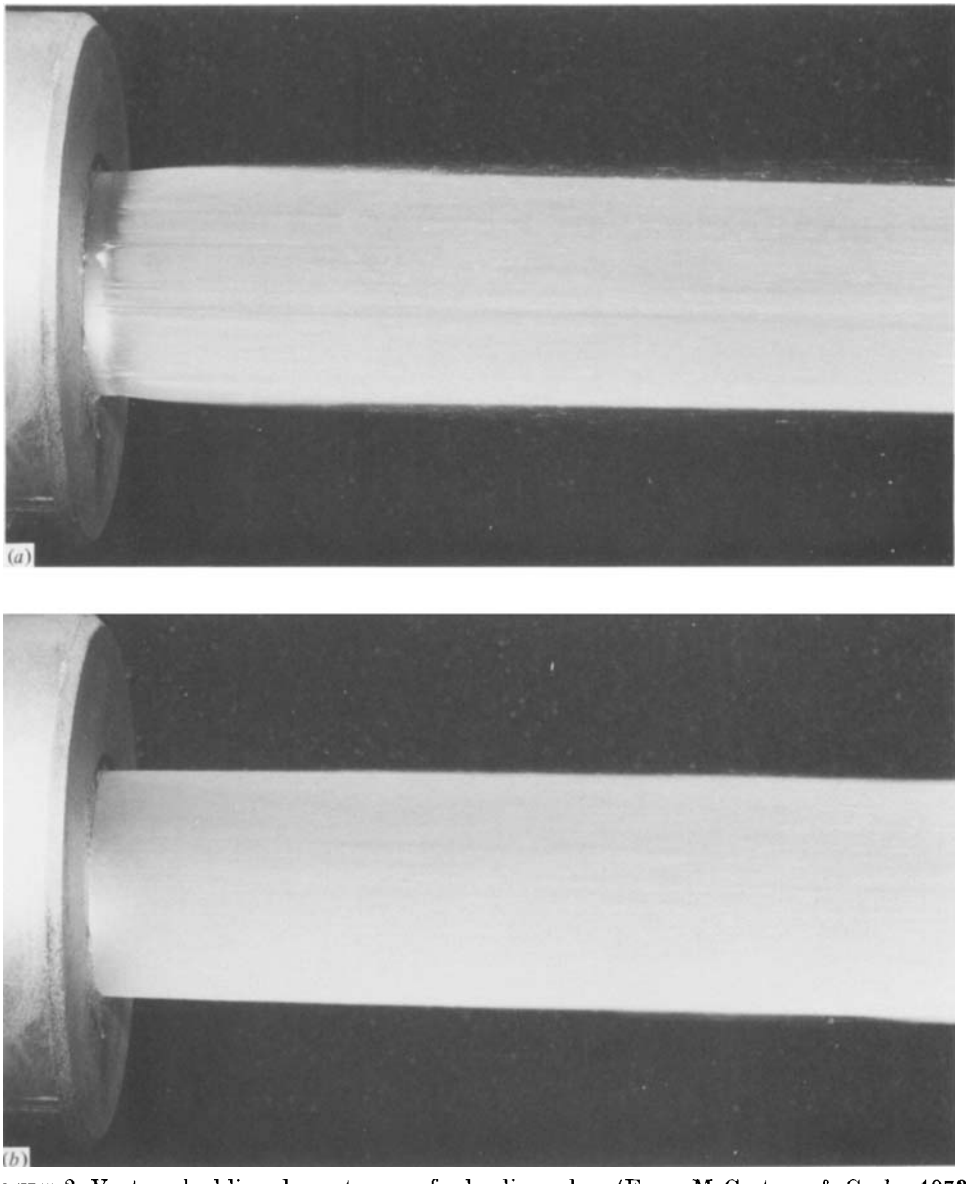

FIGURE 2. Vortex shedding downstream of a leading edge. (From McCartney & Grebe 1973.)

flat plate embedded in an unstable mean flow. It could happen that nonlinear and viscous effects will trigger an instability wave in the downstream flow in order to eliminate the singularity in unsteady pressure that the incident disturbance would otherwise produce.

But it turns out that, *unlike the solution of the corresponding trailing-edge problem*, the solution to the present problem that is non-singular at the edge is also non-causal! This occurs because the resulting formula involves a spatially growing instability wave that propagates towards the edge on the upstream mean flow. But this instability is never unbounded and decays to zero at upstream infinity. Of course the solution that does not involve the *downstream* instability wave is also non-causal.

Now it is possible to construct a causal solution to this problem, which *does not* involve an instability on the upstream flow but which, like the non-singular solution, is coupled to an instability wave that propagates away from the edge on the downstream flow. However, this solution is again *singular* at the edge!

Since it is still not clear that the causal solution will always provide the best representation of a real flow that was initiated in the distant past, I do not think we can completely rule out the non-singular solution. I shall therefore discuss the implications of both these solutions.

In §2.1 we construct an inviscid solution for the unsteady flow that occurs when an unsteady harmonic disturbance is incident on the leading edge of a plate placed in the parallel shear flow depicted in figure 1. We require that this solution be bounded at large distances from the edge. It turns out that it must then have a singularity at the edge and that it must also be non-causal. We next construct (in §2.2) an eigensolution to this problem, which is associated with a spatially growing Helmholtz instability of the downstream semi-bounded flow and which also has a singularity at the edge. The general solution to the problem is given by the sum of the particular solution constructed in §2.1 and an arbitrary multiple of this eigensolution. As we already indicated, Crighton & Leppington (1974) used a similar decomposition for their trailing edge problem. In §2.3 we show that the arbitrary multiplicative constant can always be chosen so that the leading edge singularity is eliminated from the solution. Of course, depending on such things as the viscosity, frequency, etc. the leading-edge singularity in the actual flow may not be completely eliminated by the instability wave and some flow separation might even occur.

We begin §2.4 by giving a formal derivation of the least singular causal solution. We then show that the result could also have been obtained by appropriately adjusting the arbitrary constant in the general solution alluded to above. This choice of the constant eliminates the *upstream* instability wave from the solution but not the downstream instability. In §3 we discuss the general properties of the two solutions described above and consider their relative merits. It is pointed out that they both predict the odd symmetry between the upper and lower surface instability waves that is evident in the photographs of figure 2. Formulae for the acoustic radiation are derived in §4. When the frequency goes to zero, the causal result becomes identical to the result with no edge singularity (i.e. the edge singularity disappears in this limit, Goldstein 1979, appendix B) and both results are consistent with the low-frequency solution obtained by Goldstein (1978, 1979).

In §5 we obtain specific formulae for a slug flow model of the shear layer. Their implications are discussed in §6. The calculations described in this section show that the plate does not substantially inhibit the growth rate of the downstream unstability wave until the reduced frequency, based on the distance between the plate and the edge of the shear layer, becomes very small. (The wavelength of the instability shown in figure 2 indicates that the reduced frequency is of order one there.)

There has recently been considerable interest in the so-called receptivity problem (Morkovin 1969) which is concerned with how the instability waves that lead to turbulence are triggered by disturbances in the free stream. The present work indicates that this triggering might occur in a particularly efficient way whenever the free-stream disturbance can produce large local pressure gradients by interacting with sudden changes in boundary conditions such as those associated with an edge.

2. General analysis

We consider a long thin flat plate placed in a constant density parallel shear flow in the manner depicted in figure 1. We suppose that a two-dimensional small-amplitude harmonic motion is imposed on the flow, say for definiteness, by an incident acoustic wave with frequency $\omega > 0$, which we suppose to be large enough so that viscous effects can be neglected near the edge. Then the unsteady (x and y component) velocity and pressure fluctuations (u, v) and p, respectively, will also have the harmonic time dependence

$$(p, u, v) = (\tilde{p}e^{-i\omega t}, \tilde{u}e^{-i\omega t}, \tilde{v}e^{-i\omega t})$$

and will be governed by the linearized inviscid continuity and momentum equations

$$\left(-i\omega + \overline{U}\frac{\partial}{\partial x}\right)\tilde{u} + \overline{U}'\tilde{v} = -\frac{1}{\rho_0}\frac{\partial \tilde{p}}{\partial x}, \tag{2.1}$$

$$\left(-i\omega + \overline{U}\frac{\partial}{\partial x}\right)\tilde{v} = -\frac{1}{\rho_0}\frac{\partial \tilde{p}}{\partial y}, \tag{2.2}$$

$$\frac{1}{\rho_0 c_0^2}\left(-i\omega + \overline{U}\frac{\partial}{\partial x}\right)\tilde{p} + \frac{\partial \tilde{u}}{\partial x} + \frac{\partial \tilde{v}}{\partial y} = 0 \tag{2.3}$$

respectively, where $\overline{U} = \overline{U}(y)$ is the velocity of the mean flow, ρ_0 and c_0 are its assumed constant, density and speed of sound, and the prime denotes differentiation with respect to y.

Outside of the shear layer, the incident acoustic disturbance, whose velocity and pressure are denoted by u_I, v_I, and p_I, respectively, will behave like an ordinary acoustic wave on a stationary medium and its pressure will, therefore, be of the form

$$p_I \to \exp\left[ik_0(\kappa_1 x - (1-\kappa_I^2)^{\frac{1}{2}} y - c_0 t)\right] + \text{wave reflected from the shear layer} \quad \text{as} \quad y \to +\infty \tag{2.4}$$

where $k_0 \equiv \omega/c_0$, $|\kappa_I| < 1$, and $k_0\kappa_I$ is the x-component of the wavenumber of this wave which we have, for definiteness assumed to be incident from above the shear layer. Then it follows from (2.1) to (2.3) and, in particular, from the fact that their coefficients depend only on y, that at all points within the shear layer p_I and v_I must be of the form

$$p_I/\rho_0 c_0 = P_I(\kappa_I, y)\exp\left[ik_0(\kappa_I x - c_0 t)\right], \tag{2.5}$$

$$v_I = V_I(\kappa_I, y)\exp\left[ik_0(\kappa_I x - c_0 t)\right] \tag{2.6}$$

where

$$V_I = \frac{P_I'}{ik_0(1-\kappa_I M)} \tag{2.7}$$

and

$$M = M(y) \equiv U(y)/c_0. \tag{2.8}$$

We shall suppose that $M < 1$.

This solution will not, of course, satisfy the physically required boundary condition that the normal component v of the perturbation velocity vanish at the surface of the plate and we must add to it another solution, say (u_B, v_B) and p_B, which has outgoing wave behaviour at infinity and which has a y component of velocity that is equal and opposite to v_I at the surface of the plate.

Since the coefficients of the governing equations (2.1) through (2.3) depend only on y, it is natural to solve for u_B, v_B, and p_B by taking Fourier transforms with respect to x. But this operation will automatically exclude any exponentially growing instability waves that might otherwise appear unless special care is taken to include a sufficiently rich class of generalized functions into our class of allowable Fourier transforms (Rienstra 1979). This is rather difficult to do and for the present purposes it is probably best to begin with a solution that is bounded at infinity and consider its modification due to possible exponentially growing eigensolutions. We shall see that the former solution, which is regular at infinity, will then possess a square root singularity at the edge. We facilitate the imposition of the boundary condition at infinity in the usual way by assuming that k_0 has a small imaginary part that will be put equal to zero at the end of the analysis.

2.1. *Construction of solution that is regular at infinity*

In view of the above remarks we seek a solution of the form

$$p_B/\rho_0 c_0 = e^{-i\omega t}\int_{-\infty}^{\infty} e^{ikx} A_\sigma^B(k)\, P_\sigma(k,y)\, dk, \tag{2.9}$$

$$v_B = e^{-i\omega t}\int_{-\infty}^{\infty} e^{ikx} A_\sigma^B(k)\, V_\sigma(k,y)\, dk, \tag{2.10}$$

where $\sigma = U, L$ for $y \gtrless 0$. Then taking Fourier transforms of (2.1) through (2.3) and eliminating the Fourier transformed velocities from the results, we find that P_σ must satisfy

$$D^2(P'/D^2)' + [D^2 - k^2]\, P = 0, \tag{2.11}$$

where

$$D \equiv kM - k_0 \tag{2.12}$$

and that V_σ is related to this solution by

$$V = -P'/iD. \tag{2.13}$$

Finally we require that P_U, V_U remain bounded as $y \to +\infty$ and P_L, V_L exhibit similar behaviour as $y \to -\infty$. But since there is zero mean flow at infinity, these conditions imply that

$$P_U \to C_U \exp[-(k^2 - k_0^2)^{\frac{1}{2}} y] \quad \text{as} \quad y \to +\infty \tag{2.14}$$

$$P_L \to C_L \exp[(k^2 - k_0^2)^{\frac{1}{2}} y] \quad \text{as} \quad y \to -\infty \tag{2.15}$$

where C_U, C_L are constants (which we can choose independently of k) and the branch cuts of the square root are as shown in figure 3.

We can now construct the solutions u_B, v_B, and p_B by adjusting the coefficients A_σ^B to satisfy the boundary conditions along $y = 0$, which require that v_B cancel v_I on the surface of the plate and that p_B and v_B be continuous across the half line $y = 0$, $x < 0$. Then since v_I is continuous across $y = 0$ for all x, it follows from (2.6), (2.9), and (2.10) that

$$A_U^B(k)\, V_U(k,0) = A_L^B(k)\, V_L(k,0) \tag{2.16}$$

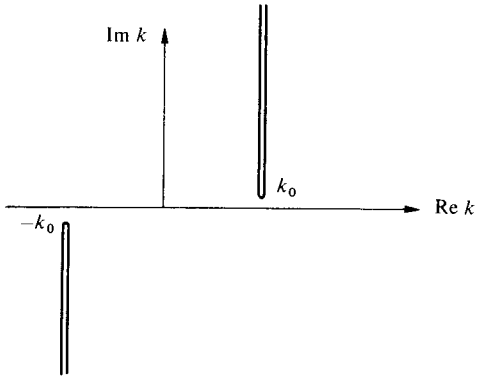

FIGURE 3. Branch cuts for $\gamma_1 = (k^2 - k_0^2)^{\frac{1}{2}}$.

and that

$$0 = \int_{-\infty}^{\infty} e^{ikx} V_U(k,0)\, A_U^B(k)\, K(k)\, dk \quad \text{for} \quad x < 0, \tag{2.17}$$

$$-V_I(\kappa_I, 0)\, e^{ik_0\kappa_I x} = \int_{-\infty}^{\infty} e^{ikx} A_U^B(k)\, V_U(k,0)\, dk \quad \text{for} \quad x > 0 \tag{2.18}$$

where

$$K(k) \equiv \frac{P_U(k,0)}{V_U(k,0)} - \frac{P_L(k,0)}{V_L(k,0)}. \tag{2.19}$$

Equations (2.17) and (2.18) can be solved by the Wiener–Hopf technique (Noble 1958, pp. 220ff). To this end we note that (2.17) implies

$$V_U(k,0)\, A_U^B(k)\, K(k) = H_-(k) \tag{2.20}$$

where $H_-(k)$ denotes a function which is analytic in the lower half k-plane. Similarly (2.18) implies that

$$V_U(k,0)\, A_U^B(k) = H_+(k) + F_-(k) \tag{2.21}$$

where $H_+(k)$ is analytic in the upper half k-plane and

$$\begin{aligned} F_- &\equiv -\frac{V_I(\kappa_I,0)}{2\pi} \int_0^{\infty} \exp\left[i(k_0\kappa_I - k)x\right] dx \\ &= \frac{V_I(\kappa_I,0)}{2\pi i(k_0\kappa_I - k)} \end{aligned} \tag{2.22}$$

is analytic in the lower half plane, since $\operatorname{Im} k_0 > 0$.

Eliminating $V_U A_U^B$ between (2.20) and (2.21) we obtain

$$H_-/K - H_+ = F_- \quad \text{for} \quad \operatorname{Im} k = 0. \tag{2.23}$$

We now suppose that K has been factored into the ratio

$$K(k) = K_+(k)/K_-(k) \quad \text{for} \quad \operatorname{Im} k = 0 \tag{2.24}$$

of two functions $K_\pm$ which are analytic and non-zero in the upper/lower half planes. Then (2.23) becomes

$$K_- H_- - H_+ K_+ = K_+ F_- \quad \text{for} \quad \operatorname{Im} k = 0. \tag{2.25}$$

Since

$$K_+(k)\,F_-(k) = \frac{V_I(\kappa_I, 0)}{2\pi i}\left[\frac{K_+(k) - K_+(k_0\kappa_I)}{k_0\kappa_I - k} + \frac{K_+(k_0\kappa_I)}{k_0\kappa_I - k}\right]$$

it follows that we can write $K_+F_- = G_- - G_+$, where $G_\pm$ are analytic in the upper/lower half planes and

$$G_- = \frac{V_I(\kappa_I, 0)}{2\pi i}\frac{K_+(k_0\kappa_I)}{k_0\kappa_I - k}. \tag{2.26}$$

Hence

$$K_-H_- - G_- = H_+K_+ - G_+; \quad \operatorname{Im} k = 0$$

and since the left-hand/right-hand side of this equation is the boundary value of a function which is analytic in the lower/upper half plane, there must be an entire function, say $E(k)$, which coincides with each of these functions in their respective half planes of analyticity. The behaviour of $H_-(k)$, and hence of $A_U^B(k)$, at $k = \infty$ is related to the behaviour of $E(k)$ at $k = \infty$. And since G_- goes to zero as $k \to \infty$, it follows that H_- and, consequently, A_U^B will possess the weakest singularity (or the most rapid decay) at $k = \infty$ when we require that $E(k) \to 0$ as $k \to \infty$. Then Liouville's theorem implies that $E(k)$ will be identically zero and therefore that

$$H_- = G_-/K_-$$

and, in view of (2.20), (2.24), and (2.26), that

$$A_U^B(k) = \frac{1}{2\pi i}\frac{V_I(\kappa_I, 0)}{V_U(k, 0)}\frac{K_+(k_0\kappa_I)}{K_+(k)}\frac{1}{k_0\kappa_I - k}.$$

Substituting this along with (2.16) into (2.9), we obtain

$$\frac{p_B}{\rho_0 c_0} = \frac{e^{-i\omega t}}{2\pi i}\int_{-\infty}^{\infty} e^{ikx}\frac{V_I(\kappa_I, 0)}{(k_0\kappa_I - k)}\frac{K_+(k_0\kappa_I)}{K_+(k)}\frac{P_\sigma(k, y)}{V_\sigma(k, 0)}\,dk \tag{2.27}$$

where

$$\sigma = U, L \quad \text{for} \quad y \gtrless 0.$$

Hence it follows from (2.19) and (2.24) that

$$\Delta p_B(x) \equiv p_B(x, 0+) - p_B(x, 0-) = \frac{\rho_0 c_0 V_I(\kappa_I, 0)\, e^{-i\omega t}}{2\pi i}\int_{-\infty}^{\infty} e^{ikx}\frac{K_+(k_0\kappa_I)}{K_-(k)}\frac{dk}{k_0\kappa_I - k}. \tag{2.28}$$

The behaviour of $\Delta p_B(x)$ at $x = 0$ is determined by the behaviour of the integrand as $k \to \infty$. Now we have shown in appendix B that $K_- \sim k^{-\frac{1}{2}}$ as $k \to \infty$. It therefore follows from the theory of Fourier transforms (Roos 1969, pp. 148 and 149) that

$$\Delta p_B(x) \sim \frac{1}{x^{\frac{1}{2}}} \quad \text{as} \quad x \to 0+. \tag{2.29}$$

Since we have selected the solution whose Fourier transform has the most rapid algebraic decay as $k \to \infty$, (2.29) represents the weakest singularity that can exist at the leading edge. This is, of course, not very surprising since the same singularity is known to occur when the edge is embedded in a uniform flow and we should not expect the non-uniform mean flow to change the local character of the solution. However, the verification of this fact is important because of the central role that this singularity plays in the analysis.

When the mean flow is symmetric about the position $y = 0$ of the plate, the resulting symmetry of the boundary-value problem (2.11) through (2.15) implies that we can always choose the irrelevant constants C_U and C_L such that

$$\left.\begin{aligned} P_L(k,-y) &= P_U(k,y) \\ V_L(k,-y) &= -V_U(k,y) \end{aligned}\right\} \quad \text{for} \quad y > 0. \tag{2.30}$$

Then the Kernel function (2.19) becomes

$$K(k) = \frac{2P_U(k,0)}{V_U(k,0)} \tag{2.31}$$

and it follows from (2.24) that the solution (2.27) becomes

$$\frac{p_B}{\rho_0 c_0} = \frac{e^{-i\omega t}}{4\pi i}\int_{-\infty}^{\infty} e^{ikx}\frac{V_I(\kappa_I,0)}{(k_0\kappa_I - k)}\frac{K_+(k_0\kappa_I)}{K_-(k)}\frac{P_U(k,|y|)}{P_U(k,0)}\,dk \tag{2.32}$$

for symmetric mean flows.

2.2. *Construction of eigensolution*

For most velocity profiles there is a range of frequencies for which the present problem possesses one or more eigensolutions that exhibit the same singularity at the edge as the solution obtained in the previous section and which involve instability waves propagating downstream from that edge. Since we can always add an arbitrary multiple of the former solutions to the latter and still have a solution to the problem, we can use them to obtain a family of solutions to the problem. But, as we indicated in the introduction, these eigensolutions will be unbounded at downstream infinity since they are associated with a Helmholtz instability of the shear flow.

We therefore begin by considering the spatially growing Helmholtz instability waves in the two doubly infinite shear layers shown in figure 4. They correspond to the portion of the original shear flow lying above/below the plane of the plate and are bounded below/above by a wall extending from $x = -\infty$ to $x = +\infty$.

These waves can be expressed in terms of the solutions P_U, V_U and P_L, V_L to the boundary-value problems (2.11) through (2.15) as

$$\frac{p_H^\alpha}{\rho_0 c_0} = P_\alpha(k_0\kappa_\alpha^*, y)\exp\left[ik_0(\kappa_\alpha^* x - c_0 t)\right], \quad \alpha = U, L \quad \text{for} \quad y \gtrless 0, \tag{2.33}$$

$$v_H^\alpha = V_\alpha(k_0\kappa_\alpha^*, y)\exp\left[ik_0(\kappa_\alpha^* x - c_0 t)\right], \quad \alpha = U, L \quad \text{for} \quad y \gtrless 0, \tag{2.34}$$

where the eigenvalues κ_α^* are chosen such that $\operatorname{Im}\kappa_\alpha^* < 0$ and V_α satisfies the additional boundary condition

$$V_\alpha(k_0\kappa_\alpha^*, 0) = 0, \quad \alpha = U, L. \tag{2.35}$$

Since any velocity profile that varies in the general manner indicated in figure 4 will either possess an inflection point, or have a discontinuity in slope there will usually be a range of frequencies, say $0 < \omega < \omega_\alpha^*$ for $\alpha = U, L$, such that these eigenvalue problems will each possess one or more solutions. No such solutions will exist for a linear velocity profile and the solutions will exist at all frequencies for the velocity discontinuity profile (see figure 6) discussed in §5. Most smooth velocity profiles will fall somewhere in between with each cut-off frequency ω_α^* equal to some finite number (Drazin & Howard 1976, pp. 32 and ff., Betchov & Criminale 1967, pp.

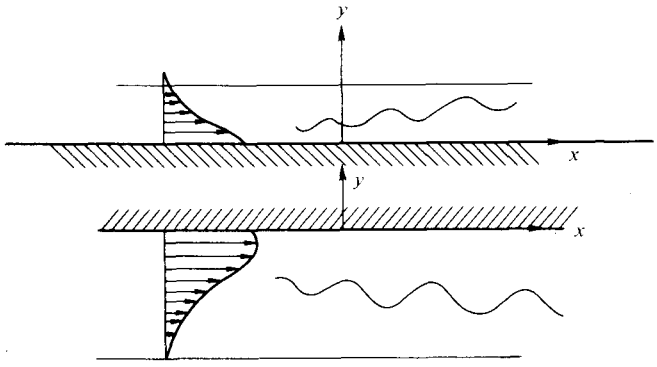

FIGURE 4. Equivalent half plane problems for instability waves.

216–219). More than one eigensolution will sometimes exist for certain, not very specific, ranges of Mach number and subranges of $0 < \omega < \omega_\alpha^*$ but we shall suppose for simplicity that there is only one such solution on each of semi-bounded flows depicted in figure 4.

Each of these solutions is, of course, defined on only half of the actual flow. We can extend them to the complete flow by setting

$$p_H^U(x,y) = v_H^U(x,y) \equiv 0 \quad \text{for} \quad y < 0$$

and

$$p_H^L(x,y) = v_H^L(x,y) = 0 \quad \text{for} \quad y > 0.$$

But the resulting functions are now discontinuous across the half line $y = 0$, $x < 0$. In order to obtain solutions which are continuous across this half line, which vanish as $y \to \pm\infty$ and still satisfy the boundary condition of zero normal velocity on the plate, we seek solutions p_E^α, v_E^α ($\alpha = U, L$) of the form

$$\left.\begin{aligned} p_E^\alpha &= p_H^\alpha + p_h^\alpha, \\ v_E^\alpha &= v_H^\alpha + v_h^\alpha, \end{aligned}\right\} \quad \alpha = U, L, \tag{2.36}$$

where p_h^α and v_h^α are solutions to the original equations which satisfy the boundary conditions

$$v_h^\alpha(x,0,t) = 0, \quad x > 0, \tag{2.37}$$

$$v_h^\alpha(x,0+,t) = v_h^\alpha(x,0-,t), \quad x < 0, \tag{2.38}$$

$$p_h^U(x,0+,t) - p_h^U(x,0-,t) = -p_H^U(x,0+,t), \quad x < 0, \tag{2.39}$$

$$p_h^L(x,0+,t) - p_h^L(x,0-,t) = +p_H^L(x,0-,t), \quad x < 0, \tag{2.40}$$

and remain bounded as $y \to \pm\infty$.

Since $p_H^U(x,0+,t)$ and $p_H^L(x,0-,t)$ remain bounded for $x < 0$, we can obtain solutions to these two boundary-value problems in the form

$$\frac{p_h^\alpha}{\rho_0 c_0} = e^{-i\omega t}\int_{-\infty}^{\infty} e^{ikx} A_\sigma^\alpha(k)\, P_\sigma(k,y)\, dk, \tag{2.41}$$

$$v_h^\alpha = e^{-i\omega t}\int_{-\infty}^{\infty} e^{ikx} A_\sigma^\alpha(k)\, V_\sigma(k,y)\, dk, \tag{2.42}$$

$\sigma = U, L$ for $y \gtrless 0$ and P_σ, V_σ are defined in §2.1. These results can be inserted into the boundary conditions (2.37)–(2.40) to obtain a set of dual integral equations which are almost identical to the set obtained in §2.1. We can then solve these equations by the Wiener–Hopf technique in the same way as we did in that section. Since the procedure is nearly the same we do not repeat it here and merely give the results

$$A_U^\alpha(k) = \frac{\mp 1}{2\pi i} \frac{P_\alpha(k_0\kappa_\alpha^*, 0\pm)}{V_U(k,0)} \frac{K_-(k_0\kappa_\alpha^*)}{K_+(k)} \frac{1}{k_0\kappa_\alpha^* - k}, \quad \alpha = U, L, \tag{2.43}$$

$$A_L^\alpha = A_U^\alpha \frac{V_U(k,0)}{V_L(k,0)}, \tag{2.44}$$

$$\Delta p_h^\alpha = p_h^\alpha(x, 0+, t) - p_h^\alpha(x, 0-, t)$$

$$= \mp \frac{P_\alpha(k_0\kappa_\alpha^*, 0\pm)}{2\pi i} e^{-i\omega t} \rho_0 c_0 \int_{-\infty}^{\infty} e^{ikx} \frac{K_-(k_0\kappa_\alpha^*)}{K_-(k)} \frac{dk}{k_0\kappa_\alpha^* - k}, \quad \alpha = U, L, \tag{2.45}$$

where the upper $+$ or $-$ sign is to be associated with $\alpha = U$ and the lower sign with $\alpha = L$, and $K_\pm$ are defined in §2.1.

It is clear that integrand in (2.45) has the same asymptotic behaviour as $k \to \infty$ as the integrand in (2.28). Hence, it follows that Δp_h^α has the same singularity at $x = 0+$ as Δp_B, that is,

$$\Delta p_h^\alpha \sim \frac{1}{x^{\frac{1}{2}}} \quad \text{as} \quad x \to 0+. \tag{2.46}$$

We have now constructed two eigensolutions with square root singularities at $x = 0$ corresponding to $\alpha = U, L$ and therefore the most general eigensolution can be expressed as a linear combination of the two, say

$$\tilde{p}_E = B^U p_E^U + B^L p_E^L \tag{2.47}$$

where B^U, B^L are constants. Then we can always introduce new constants, say β_0 and β_1, by

$$\beta_0 \equiv \frac{2[P_U(k_0\kappa_U^*, 0+) K_-(k_0\kappa_U^*) B^U - P_L(k_0\kappa_L^*, 0-) K_-(k_0\kappa_L^*) B^L]}{P_U(k_0\kappa_U^*, 0+) K_-(k_0\kappa_U^*) + P_L(k_0\kappa_L^*, 0-) K_-(k_0\kappa_L^*)} \tag{2.48}$$

and

$$\beta_1 \equiv \frac{B^U + B^L}{P_U(k_0\kappa_U^*, 0+) K_-(k_0\kappa_U^*) + P_L(k_0\kappa_L^*, 0-) K_-(k_0\kappa_L^*)},$$

and use these to eliminate B^U and B^L in (2.47) to obtain

$$\tilde{p}_E = \tfrac{1}{2}\beta_0(p_E^U - p_E^L) + \beta_1[P_L(k_0\kappa_L^*, 0-) K_-(\kappa_L^* k_0) p_E^U + P_U(k_0\kappa_U^*, 0+) K_-(k_0\kappa_U^*) p_E^L]. \tag{2.49}$$

Now it follows from (2.33), (2.36), and (2.45) that the coefficient of β_1 is an eigensolution to the problem that is non-singular at $x = 0$. It is therefore reasonable to suppose that this eigensolution will not be generated by the viscous forces at the leading edge and will therefore be decoupled from the incident disturbance. In fact, since $\kappa_L^* = \kappa_U^*$ when the shear flow is symmetric about the position $y = 0$ of the plate, it is easy to see that p_h^U, p_h^L will then make no contribution to this eigensolution which now represents an anti-symmetric spatially growing instability wave on the unbounded upstream shear flow (referred to as the varicose disturbance by Rayleigh). We therefore suppose that this eigensolution plays no role in the phenomenon under consideration and consider only the *singular* eigensolution

$$p_E = \tfrac{1}{2}\beta_0(p_E^U - p_E^L). \tag{2.50}$$

The corresponding upwash velocity v_E is, of course, given by

$$v_E = \tfrac{1}{2}\beta_0(v_E^U - v_E^L). \tag{2.51}$$

We shall subsequently show that the symmetry exhibited by the instability waves in figure 2 is consistent with the first eigensolution in (2.49) and *not* with the neglected eigensolution.

When the mean velocity profile is asymmetric about $y = 0$ so that the upper and lower velocity profile cut-off frequencies ω_U^*, ω_L^* are unequal, there will be a range of frequencies, say

$$\omega_L^* < \omega < \omega_U^*$$

when $\omega_L^* < \omega_U^*$, where this uniqueness problem does not arise. In this case only the upper flow will possess an instability wave corresponding to the boundary value problems (2.33) through (2.35) and there will therefore be only one eigensolution, which will, of course, still have a square root singularity at the edge. No eigensolutions will exist for ω in the range

$$\max\{\omega_L^*, \omega_U^*\} < \omega < \infty.$$

When the mean flow is symmetric about the position $y = 0$ of the plate $\omega_U^* = \omega_L^* \equiv \omega^*$ and

$$\kappa_L^* = \kappa_U^* \equiv \kappa^*, \tag{2.52}$$

say. Then we can insert (2.43) and (2.44) into (2.41), insert the result together with (2.30), (2.31), (2.33), and (2.52) into (2.36) and finally insert this result into (2.50) to obtain

$$\frac{p_E}{\rho_0 c_0} = -\frac{e^{-i\omega t}}{4\pi i}\int_{-\infty}^{\infty} e^{ikx}\frac{V_I(\kappa_I, 0)}{(k_0\kappa^* - k)}\frac{K_+(k_0\kappa_I)}{K_-(k)}\frac{P_U(k, |y|)}{P_U(k, 0)}\,dk$$
$$+ \tfrac{1}{2}\beta \exp\left[ik_0(\kappa^* x - c_0 t)\right] P_U(k_0\kappa^*, |y|), \quad 0 < \omega < \omega^* \tag{2.53}$$

where we have put

$$\beta \equiv \frac{K_+(k_0\kappa_I)\, V_I(\kappa_I, 0)}{K_-(k_0\kappa^*)\, P_U(k_0\kappa^*, 0+)} \tag{2.54}$$

and have for convenience set the unessential normalizing constant β_0 equal to β. The general solution (p_G, v_G) to the boundary-value problem is given by

$$p_G = p_B + Cp_E, \quad v_G = v_B + Cv_E, \tag{2.55}$$

where C is an arbitrary constant and (p_B, v_B) is the particular solution constructed in §2.1.

2.3. *Construction of non-singular solution and determination of instability amplitude*

The general solution (2.55) will usually be unbounded at infinity and singular at the leading edge. However, we can eliminate the leading edge singularity by choosing the arbitrary constant C so that

$$\Delta p_B \to -C\Delta p_E \quad \text{as} \quad x \to +0 \quad \text{for} \quad 0 < \omega < \min\{\omega_U^*, \omega_L^*\}.$$

We consider only the case of a symmetric mean flow. Then it follows from (2.30),

(2.28), and (2.53) that this occurs when $C = 1$. Hence, it follows from (2.32), (2.53), and (2.55) that the solution p_F which is non-singular at the edge is given by

$$\frac{p_F}{\rho_0 c_0} = \frac{e^{-i\omega t}}{4\pi i}\int_{-\infty}^{\infty} e^{ikx}\frac{V_I(\kappa_I,0)}{(k_0\kappa_I - k)}\frac{K_+(k_0\kappa_I)}{K_-(k)}\left[\frac{k_0(\kappa^* - \kappa_I)}{(k_0\kappa^* - k)}\right]\frac{P_U(k,|y|)}{P_U(k,0)}\,dk$$

$$+\frac{\beta}{2}\exp\left[ik_0(\kappa^* x - c_0 t)\right]P_U(k_0\kappa^*, |y|) \quad \text{for} \quad 0 < \omega < \omega^*. \tag{2.56}$$

Only the second term of this solution grows exponentially large at downstream infinity. We can therefore think of it as the Helmholtz instability wave triggered at the leading edge by the incident acoustic wave p_I (given by (2.5)). A suitable measure of the strength of the instability produced at the edge by a particular type of acoustic disturbance is then the amplitude of this term at (actually just above) the leading edge divided by the amplitude of the acoustic wave at this point, that is,

$$\mathscr{A}_F(\kappa_I, \kappa^*) \equiv |(\text{2nd term of (2.56)})/p_I(0,0,t)| = \tfrac{1}{2}|\beta P_U(k_0\kappa^*, 0)/P_I(\kappa_I, 0)|.$$

Using (2.54) we obtain

$$\mathscr{A}_F(\kappa_I, \kappa) \equiv \frac{1}{2}\left|\frac{K_+(k_0\kappa_I)}{K_-(k_0\kappa)}\frac{V_I(\kappa_I,0)}{P_I(\kappa_I,0)}\right|. \tag{2.57}$$

2.4. *The causal solution and the upstream instability wave*

As indicated in the introduction, the real time solutions obtained by taking the inverse Laplace transform of the non-singular solution (2.56) or of the solution (2.32), which is bounded at infinity, will not be causal, that is, the diffracted field will anticipate the initial incident disturbance when the process is first started. The easiest way to obtain a causal solution to the present problem is (Briggs 1964, cha. 2; Tam 1971) to first solve the problem for the case where the frequency ω is complex and has a large positive imaginary part. The causal solution for real ω is then obtained as the analytic continuation of this solution to the real axis in the complex ω plane.

To this end we first construct a solution of the scattering problem that has complex frequency and is bounded at infinity. The procedure is the same as the one used for the real frequency case in §2.1 and the result is formally identical to the previous solution which is given by (2.27) (or by (2.32) for the case of a symmetrical near flow). In fact the only difference between the two solutions is that some of the complex zeros that appear in the numerator and denominator of the Kernel function (2.19) will lie in different half planes in the two cases and the factorizing functions $K_\pm$ will therefore have to be different in the two cases.

We shall for simplicity restrict our attention to the case where the mean flow is symmetric about the position $y = 0$ of the plate and the frequency ω is less than the cut-off frequency ω^* of the half-space Helmholtz instability of the downstream flow. Then the non-causal bounded solution will be given by (2.32) and its Kernel function K will be given by (2.31).

Equations (2.31), (2.35), and (2.52) show that K has a simple pole at $k = k_0\kappa^*$, which is associated with the downstream instability wave. But there is also a Helmholtz instability wave on the upstream jet velocity profile which for the present symmetric case must be given by (2.33) and (2.34) with the boundary condition (2.35) replaced by

$$P_U(k_0\kappa_J, 0) = 0, \tag{2.58}$$

where κ_J is now used in place of κ^* to denote the eigenvalue of this new eigenfunction problem.† When ω is real this instability wave will propagate in the downstream direction and grow exponentially fast in that direction. For most profiles it will only exist for a certain range of frequencies, say

$$0 < \omega < \omega_J,$$

where in all cases of which I am aware the sinuous disturbance cut-off frequency ω_J is larger than or equal to the cut-off frequency ω^* for the half-space instability.

The Kernel function (2.31) will therefore have a simple complex zero at $k = k_0\kappa_J$ in addition to its pole at $k = k_0\kappa^*$ for $0 < \omega < \omega^*$. These two singularities must of course lie in the lower half k-plane when ω is real but they will move into the upper half plane when the imaginary part of ω is sufficiently large and positive.‡ The factorization

$$K(k) = K_+^\dagger(k)/K_-^\dagger(k), \quad \operatorname{Im} k = 0, \quad -\infty < \operatorname{Re} k < \infty \tag{2.59}$$

of the Kernel function (2.31) into the two functions $K_\pm^\dagger$ that are analytic in the upper/lower half planes will therefore differ in the present case from the factorization (2.24) of §2.1. In fact, since the remaining zeros, poles and branch points of K, that is, all those not associated with the instability waves, must lie in the same half planes in both cases, the present factorizing functions $K_\pm^\dagger$ are related to those of §2.1 (i.e. $K_\pm$) by§

$$K_\pm^\dagger(k,\omega) = K_\pm(k,\omega)\left(\frac{k-k_0\kappa^*}{k-k_0\kappa_J}\right) \tag{2.60}$$

where $K_\pm(k,\omega)$ are the functions of §2.1 extended to complex values of ω with large imaginary part.

The solution to the present problem which we denoted by (p_C, v_C) is therefore given by (2.32) with $K_\pm$ replaced by $K_\pm^\dagger$. Hence, it follows from (2.60) that

$$\frac{p_C}{\rho_0 c_0} = \frac{e^{-i\omega t}}{4\pi i}\int_{-\infty}^{\infty} e^{ikx}\frac{V_I(\kappa_I,0)}{(k_0\kappa_I - k)}\frac{K_+(k_0\kappa_I)}{K_-(k)}\left(\frac{\kappa_I-\kappa^*}{\kappa_I-\kappa_J}\right)\left(\frac{k-k_0\kappa_J}{k-k_0\kappa^*}\right)\frac{P_U(k,|y|)}{P_U(k,0)}\,dk. \tag{2.61}$$

This result only applies when the imaginary part of ω is sufficiently large. Its analytic continuation to values of ω with small imaginary part is obtained by deforming the integration contour so that it is not crossed by any singularities as $\operatorname{Im}\omega \to 0$. But since the zero at $k_0\kappa_J$ arising from $P_U(k,0)$ is cancelled by the zero in

† We have already indicated that, for the symmetric mean flow under consideration, the instability wave (2.33) on the semi-bounded downstream flow can also exist on the upstream flow where it represents an antisymmetric instability mode (Betchov & Criminale 1967, pp. 218 and 219). The instability wave corresponding to κ_J represents a symmetric instability mode (mode I in figure 53.3 of Betchov & Criminale) called the sinuous disturbance by Rayleigh.

‡ We cannot of course prove that this will be the case for every velocity profile, but Hardisty (1974) has shown it to be true for the slug flow profile considered in §5 below and we have found it to be true for the incompressible jet studied in §53 of Betchov & Criminale (1967) (note their figure 53.1).

§ Recall that the solution of §2.1 was constructed on the assumption that ω had a small positive imaginary part that was eventually put equal to zero. However, the functional form of that solution cannot change as the magnitude of the imaginary part of ω is increased until it becomes large enough to cause the poles and zeros associated with the instability waves to cross the real axis. All this is easily verified for the specific Kernel functions (5.13) corresponding to the slug flow jet.

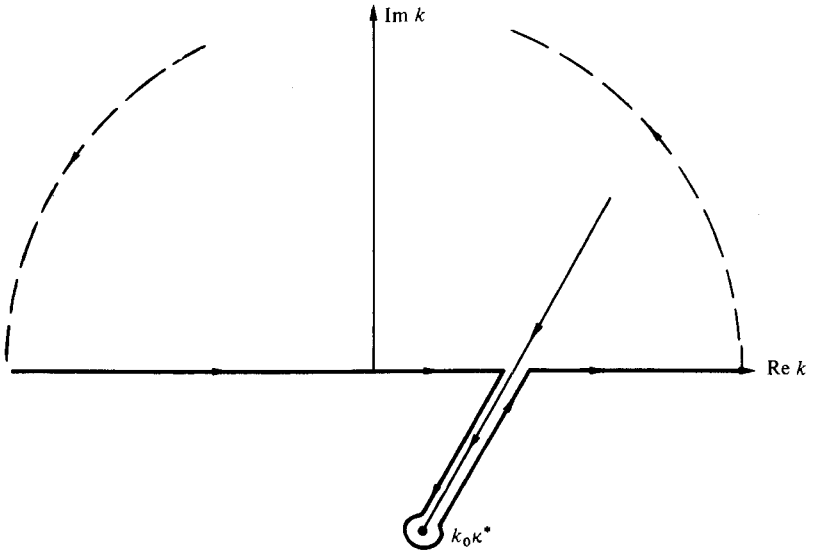

FIGURE 5. Integration contour for causal solution.

the numerator of (2.61), the only singularity that crosses the real axis during this limit is the simple pole at $k_0\kappa^*$. The integration contour for $x > 0$ can therefore be taken as shown in figure 5. Then applying the method of residues to evaluate the contribution of the pole at $k_0\kappa^*$, we obtain upon using (2.54)

$$\frac{p_C}{\rho_0 c_0} = \frac{e^{-i\omega t}}{4\pi i}\int_{-\infty}^{\infty} e^{ikx}\frac{V_I(\kappa_I,0)}{(k_0\kappa_I-k)}\frac{K_+(k_0\kappa_I)}{K_-(k)}\left(\frac{\kappa_I-\kappa^*}{\kappa_I-\kappa_J}\right)\left(\frac{k-k_0\kappa_J}{k-k_0\kappa^*}\right)\frac{P_U(k,|y|)}{P_U(k,0)}\,dk$$
$$+\frac{\beta}{2}\left(\frac{\kappa^*-\kappa_J}{\kappa_I-\kappa_J}\right)\exp\left[ik_0(\kappa^* x-c_0 t)\right]P_U(k_0\kappa^*,|y|) \quad \text{for} \quad 0<\omega<\omega^*. \tag{2.62}$$

The derivation of this result is of course only formal since we were not able to explicitly verify the relation (2.60) for all velocity profiles. However, it does represent a solution to the scattering problem formulated in §2.1, which (as we shall show in the next section) is decoupled from the instability of the upstream flow. And, as implied in the introduction, I believe this maybe more physically significant than causality.

In order to show that (2.62) is a solution, notice that

$$\frac{1}{(k_0\kappa_I-k)}\left(\frac{\kappa_I-\kappa^*}{\kappa_I-\kappa_J}\right)\left(\frac{k-k_0\kappa_J}{k-k_0\kappa^*}\right)=\frac{1}{k_0\kappa_I-k}-\left(\frac{\kappa^*-\kappa_J}{\kappa_I-\kappa_J}\right)\frac{1}{(k_0\kappa^*-k)}.$$

Hence it follows from (2.32) and (2.53) that (2.62) is a special case of the general solution (2.55), which corresponds to setting the constant C equal to $(\kappa^*-\kappa_J)/(\kappa_I-\kappa_J)$. It must therefore itself be a solution.

We have seen that it is also the causal solution for the special case of the slug flow velocity profile discussed in §5. We therefore expect that it will also represent the causal solution for most smooth velocity profiles at frequencies below the cut-off frequency for the half space instability on the downstream semi-bounded flow.

As in the case of the non-singular solution, (2.62) is coupled to the Helmholtz

instability on the downstream semi-bounded flow. But in this case the ratio $\mathscr{A}_C(\kappa_I, \kappa^*)$ of the amplitude of the instability wave at the leading edge divided by the amplitude of the acoustic wave at that point is related to the corresponding ratio $\mathscr{A}_F(\kappa_I, \kappa^*)$ for the non-singular solution by

$$\mathscr{A}_C(\kappa_I, \kappa^*) = \mathscr{A}_F(\kappa_I, \kappa^*) \left| \left(\frac{\kappa^* - \kappa_J}{\kappa_I - \kappa_J} \right) \right|. \tag{2.63}$$

3. General discussion and comparison of solutions

We have now obtained three different solutions to the leading-edge scattering problem for a symmetric mean flow and ω in the range $0 < \omega < \omega^*$, where we have assumed that the cut-off frequency ω^* for the instability of semi-bounded downstream flow is always less than or equal to the cut-off frequency ω_J of the sinuous instability of the upstream flow. The solution (2.32), which we denote by p_B, is bounded at infinity, has a square-root singularity at the leading edge, and is non-causal. It holds for all values of ω. The solution (2.56), which we denote by p_F, is unbounded at infinity but is non-singular at the leading edge and is non-causal. The unboundedness results from the triggering of an instability on the downstream semi-bounded flow so that this solution only exists for ω less than the cut-off frequency ω^* of this wave. The causal solution (2.62), which we denote by p_C, is also unbounded at infinity due to the triggering of an instability wave on the downstream flow but, as can easily be seen by an argument similar to the one preceding (2.29), it has a square-root singularity at the leading edge. Thus unlike the case of a trailing edge, the solution which is bounded at a leading edge *does not coincide* with the causal solution!

The flow is completely stable when $\omega > \omega_J$ and the solution that is bounded at infinity is then also causal! For $\omega < \omega^*$ the non-causal solutions (2.32) and (2.56) both involve the sinuous instability wave of the upstream flow. This wave decays to zero at upstream infinity and reaches a finite value at the edge. It is not of course present in the downstream region. Mathematically, it arises from the pole in the integrands of (2.32) and (2.56) that occurs because κ_J must satisfy (2.58). When $x < 0$, the contour integrals are closed in the lower half k-plane and the contribution of this pole is just the upstream sinuous instability wave. This pole is cancelled out by a corresponding zero in the numerator of the causal solution (2.62). Thus, as one would expect, the causal solution only involves instability waves propagating away from the edge. But since disturbances can propagate upstream on a subsonic flow, it is possible (though rather unlikely, I feel) that the upstream instability wave could be triggered by the unsteady motion occurring at the edge – especially if this instability wave were to decay very rapidly as $x \to -\infty$. However, it can be shown (Drazin & Howard 1966) that the decay rate $\operatorname{Im} k_0 \kappa_J$ of this mode gives to zero as $\omega\delta/U_{\max} \to 0$, where δ is some characteristics width of the jet.

It is worth considering the behaviour of the causal solution for ω in the range $\omega^* < \omega < \omega_J$. The downstream flow will now be stable and the non-singular solution (2.62) will no longer exist while the causal solution will no longer be given by (2.61). Although this cannot be proved in general and I have not investigated the possibility for any particular mean flow, it is likely that the only singularity or zero that can cross the real axis of the k-plane as $\operatorname{Im} \omega \to \infty$ is the one at $k_0 \kappa_J$. Then two possibilities can occur: either $k_0 \kappa_J$ will remain in the lower half plane and the causal solution will

coincide with the solution p_B (given by (2.32)) or $k_0\kappa_J$ will move into the upper half plane and the integrand of the causal solution will differ from that of (2.32) by the factor $(k-k_0\kappa_J)$. In which case an argument similar to the one preceding (2.29) will show that this solution must become infinite like $x^{-\frac{3}{2}}$ at the leading edge. It therefore appears that the causal solution will either contain an instability wave propagating *toward* the edge, which is very unlikely behaviour for a causal solution, or it will involve a non-integrable singularity at the edge.

When ω is in the range $0 < \omega < \omega^*$, the unbounded solutions (2.56) and (2.62) are both special cases of the general solution (2.55). The non-singular solution (2.56) is obtained by adjusting its arbitrary constant to eliminate the edge singularity and the causal solution is obtained by adjusting it to eliminate the contribution from the upstream instability. Both solutions are therefore coupled to the downstream instability wave (2.33) and (2.34).

Now the vortex shedding shown in figure 2 is, of course, highly nonlinear, but we might still expect these equations to provide a fairly good representation of the flow in the vicinity of the edge where the amplitude of the unsteady motion is not too large. Equation (2.30) implies that the axial velocities associated with the upper surface instability wave in the singular eigensolution (2.54) will be 180° out of phase from those associated with the lower surface instability wave. Then whenever the lower surface motion is in the upstream direction the upper surface motion at the corresponding position will be in the downstream direction. The lower photograph in figure 2 clearly shows that the lower surface vortical motion is in the upstream direction near the leading edge (where the linear solution applies) while the upper surface motion appears to be in the downstream direction.

4. The diffracted radiation

Since $\operatorname{Im}\kappa^* < 0$ and $\operatorname{Re}\kappa^* > 0$, it is easy to see that the terms associated with the downstream Helmholtz instability do not contribute to the pressures given by (2.56) and (2.62) when the observation point y lies far above the plate (i.e. in the radiation field) and $\theta \equiv \tan^{-1} y/x$ lies outside the range

$$0 < \theta < \tan^{-1} - \operatorname{Im}\kappa^*/\operatorname{Re}\kappa^*. \tag{4.1}$$

The pressure in the radiation field is therefore determined by the integral terms which can be evaluated for large values of $r \equiv (x^2+y^2)^{\frac{1}{2}}$ by the method of stationary phase. Our interest here lies in the diffracted wave. We therefore neglect the contribution of the poles, which correspond to the reflected wave, to obtain upon inserting (2.14) into (2.32), (2.56), and (2.62), applying the method of stationary phase, and using (2.5) and (2.57) to simplify the result

$$|p_\lambda/p_I(0,0,0)| \sim (2\pi r k_0)^{-\frac{1}{2}} \left| \frac{C_U \mathscr{A}_F(\kappa_I, \cos\theta)}{P_U(k_0\cos\theta, 0)\,(\kappa_I - \cos\theta)} \right| T_\lambda(\theta) \quad \text{as} \quad r \to \infty;$$
$$\theta > \tan^{-1}(-\operatorname{Im}\kappa^*/\operatorname{Re}\kappa^*), \quad 0 < \omega < \omega^*, \quad \text{for} \quad \lambda = B, F, \text{ or } C, \tag{4.2}$$

where

$$T_\lambda = \begin{cases} 1 & \text{for} \quad \lambda = B \\ \left| \dfrac{\kappa^* - \kappa_I}{\kappa^* - \cos\theta} \right| & \text{for} \quad \lambda = F \\ \left| \dfrac{\kappa^* - \kappa_I}{\kappa_J - \kappa_I} \right| \left| \dfrac{\kappa_J - \cos\theta}{\kappa^* - \cos\theta} \right| & \text{for} \quad \lambda = C \end{cases} \tag{4.3}$$

and $\mathscr{A}_F(\kappa_I, \kappa)$ is defined by (2.57). This result holds for all frequencies and angles for the solution p_B that is bounded at infinity and, as we have seen in §3, the causal solution becomes identical to p_B when $\omega > \omega_J$ while the non-singular solution p_F does not exist when $\omega > \omega^*$.

Since† $\kappa_J \to \infty$ while κ^* remains finite‡ as $\omega\delta/\sigma_{\max} \to 0$ (Drazin & Howard 1966) it follows from (4.3) that $T_C \to T_F$ as $\omega\delta/U_{\max} \to 0$ and therefore that the causal and non-singular solutions have the same acoustic field in this limit.

The complete low frequency limits of these results are rather subtle since the straightforward approximation to the Kernel function, which determines the $K_\pm(k)$ functions that appear in $\mathscr{A}_F$, is not uniformly valid for all values of k (Rienstra 1979). I will not go into detail here (the interested reader is referred to Rienstra) but the net effect of the non-uniformity is to introduce a factor of

$$\left|\frac{\kappa^* - \cos\theta}{\kappa^* - \kappa_I}\right|$$

which cancels the ones that appear in the solutions that are coupled to the downstream instability. The result is that the low-frequency approximation to these solutions will vary with angle like

$$[1 - M(0)\cos\theta]^{-1}\left[1 - \frac{1}{\kappa_I}\cos\theta\right]^{-1},$$

where $M(y)$ is the Mach number of the jet defined by (2.8). This is in *complete agreement* with Goldstein's (1978, 1979) low frequency solution for the scattering of a vortical disturbance by a leading edge. (In this latter case κ_I corresponds to the wavenumber $1/M(y)$ of the incident vortical disturbance.) It is worth noting that Goldstein's result is in excellent agreement with experiment.

The issue of causality was not explicitly discussed by Goldstein (1978, 1979). But only the low- and high-frequency limits were treated there and we have seen that causality is irrelevant in the high-frequency limit. In order to understand the low frequency limit, we note that the imposition of causality can be thought of as a procedure for putting in the correct damping in order to ensure that the instability waves travel away from the point where they are generated. But since the downstream instability waves do not actually grow in the low frequency limit (and, in fact, become purely convected disturbances), the small damping already included by Goldstein to deal with the other waves also causes the instability waves to travel in the proper direction and consequently yields the same result as the imposition of causality.

5. Plug flow model

Evaluation of the results of the previous sections requires the solution of the ordinary differential equation (2.11). For most velocity profiles, this must be done numerically, but relatively simple results can be obtained for the discontinuous or slug flow velocity profile shown in figure 5, since (2.11) will then have constant coefficients and will therefore be quite easy to solve. This profile is somewhat singular

† But, as we have already indicated, $k_0\kappa_J \to 0$ in this limit.

‡ In fact $\kappa^* \to 1/M$ in this limit, so it turns into a convected disturbance which does not grow as it propagates downstream.

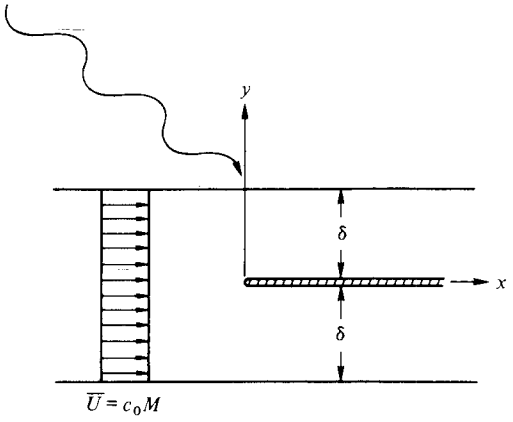

FIGURE 6. Slug flow model of shear flow.

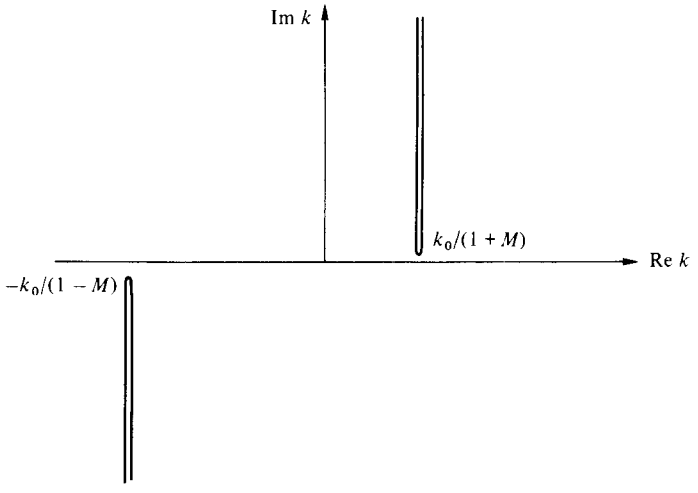

FIGURE 7. Branch cuts for $\gamma(k,y)$ and $\gamma_2 = (k^2-(Mk-k_0)^2)^{\frac{1}{2}}$.

however, in that the cut-off frequencies are infinite for both the sinuous instability on the upstream flow and the Helmholtz instability on the semi-bounded downstream flow.

An alternative approach that avoids this difficulty, is to approximate the solutions to (2.11) by their low and high frequency asymptotic expansions. But since, as was shown in §3, the causal solution becomes decoupled from the instability waves in the high frequency limit and, in fact, becomes identical to the bounded solution, I decided to adopt the former approach. However, the reader should use a certain amount of care when interpreting the results.

We suppose that the plate is located at the centre of the region of non-zero mean flow whose width is 2δ (see figure 6). Then within this region, which we denote as region 2, the general solution of (2.11) is simply

$$P = Ae^{\gamma_2(k)y} + Be^{-\gamma_2(k)y}, \tag{5.1}$$

where A and B are constants and

$$\gamma_2(k) \equiv (k^2-(k_0-kM)^2)^{\frac{1}{2}}, \tag{5.2}$$

where, for definiteness, the branch of the square root is as indicated in figure 7.

In the exterior of region 2, where there is no mean flow, the bounded solutions are of the form

$$P = \text{constant} \times e^{\mp y\gamma_1(k)}, \quad y \gtrless 0, \tag{5.3}$$

where

$$\gamma_1(k) \equiv (k^2-k_0^2)^{\frac{1}{2}} \tag{5.4}$$

with the branch chosen as indicated in figure 3.

Since continuity of pressure and particle displacement must be imposed at the boundary of region 2, these solutions must satisfy the jump conditions (Goldstein 1976, p. 20).

$$P(\pm\delta\pm 0) = P(\pm\delta\mp 0), \tag{5.5}$$

$$(k_0-Mk)^2P'(\pm\delta\pm 0) = k_0^2P'(\pm\delta\mp 0) \tag{5.6}$$

along these lines.

5.1. *Calculation of particular solutions*

It is easy to show with a little algebra that the solutions corresponding to P_U and P_L, which are only required to satisfy the boundary conditions (2.14) and (2.15), can be written as

$$P_U = \begin{cases} e^{-\gamma_1(k)y}, & y \geqslant \delta, \\ \dfrac{e^{-\gamma_1(k)\delta}}{2\gamma_2(k)k_0^2}[A^+(k)\,e^{-\gamma_2(k)y} - A^-(k)\,e^{\gamma_2(k)y}], & 0 \leqslant y \leqslant \delta, \end{cases} \tag{5.7}$$

$$P_L = \begin{cases} \dfrac{e^{-\gamma_1(k)\delta}}{2\gamma_2(k)k_0^2}[A^+(k)\,e^{\gamma_2(k)y} - A^-(k)\,e^{-\gamma_2(k)y}], & -\delta \leqslant y \leqslant 0, \\ e^{\gamma_1(k)y}, & y \leqslant \delta, \end{cases} \tag{5.8}$$

where

$$A^\pm(k) \equiv [\gamma_1(k)\,(k_0-Mk)^2 \pm \gamma_2(k)\,k_0^2]\,e^{\pm\gamma_2(k)\delta} \tag{5.9}$$

and we have taken the unessential constants C_U, C_L to be unity.

The solution corresponding to the incident acoustic wave p_I, which is defined by the boundary condition (2.4), must behave like

$$e^{\gamma_1(k_0\kappa_I)y} + Re^{-\gamma_1(k_0\kappa_1)y}$$

above the region of mean flow, like (5.1) with $k = k_0\kappa_I$ within the region of mean flow and like (5.3) with $k = k_0\kappa_I$ below this region.

It is again easy to show with a little algebra that the solution that satisfies (5.5) and (5.6) is given by

$$P_I = \frac{2\gamma_1(k_0\kappa_I)\,k_0^2(1-M\kappa_I)^2\,e^{\gamma_1(k_0\kappa_I)\delta}}{[A^+(k_0\kappa_I)]^2-[A^-(k_0\kappa_I)]^2} \\ [A^+(k_0\kappa_I)\,e^{\gamma_2(k_0\kappa_I)y} - A^-(k_0\kappa_I)\,e^{-\gamma_2(k_0\kappa_I)y}] \quad \text{for} \quad -\delta \leqslant y \leqslant \delta. \tag{5.10}$$

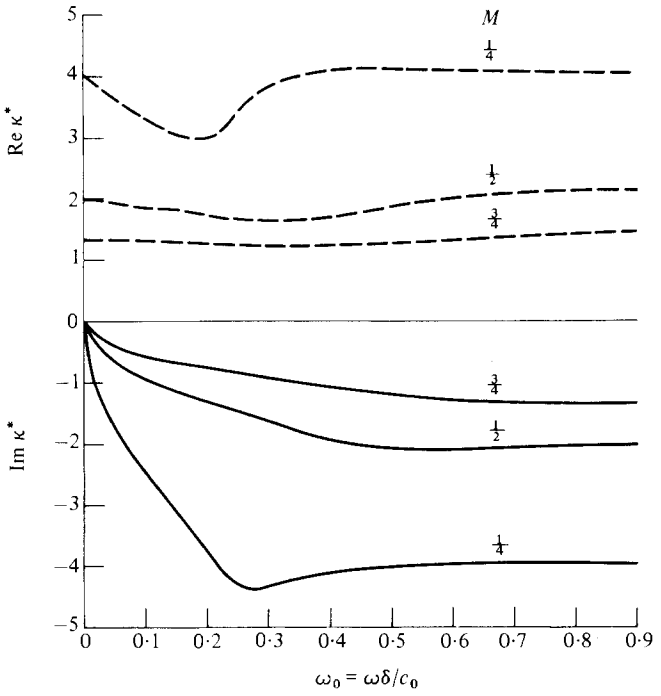

FIGURE 8. Eigenvalues for Kelvin–Helmholtz instability on semi-bounded downstream flow, real part shown dashed.

Since the mean flow is symmetric, equation (2.52) must hold and there will only be a single eigenvalue κ^* for the instability wave on the semi-bounded downstream flow, which is given by (2.33) subject to the boundary condition (2.35). For the slug flow model which we are now considering, P_α (for $\alpha = U, L$) is given by (5.7) and (5.8). Hence, it follows from (2.13) and (2.35) that we must put $A^+ = -A^-$ and therefore that κ^* must be a root of

$$\gamma_1(k_0\kappa^*)(1-M\kappa^*)^2+\gamma_2(k_0\kappa^*)\tanh\delta\gamma_2(k_0\kappa^*) = 0. \tag{5.11}$$

The eigensolution for the sinuous instability on the upstream flow is also given by (2.33) with P_α, $\alpha = U, L$, given by (5.7) and (5.8), but in this case it must satisfy the boundary condition (2.58), which implies that $A^+ = A^-$ and therefore that the eigenvalue κ_J is a root of

$$\gamma_1(k_0\kappa_J)(1-M\kappa_J)^2+\gamma_2(k_0\kappa_J)\coth\delta\gamma_2(k_0\kappa_J) = 0. \tag{5.12}$$

Equations (5.11) and (5.12) will have several roots which correspond to modes trapped in the velocity discontinuity layer that propagate upstream against the flow (Gottlieb 1959). But these equations will each have only one root corresponding to a downstream propagating instability wave that grows exponentially in that direction. Then $\mathrm{Re}\,\kappa^* \geqslant 0$, $\mathrm{Re}\,\kappa_J \geqslant 0$, and $\mathrm{Im}\,\kappa^* \leqslant 0$, $\mathrm{Im}\,\kappa_J \leqslant 0$ for these waves. Figure 7 is a plot of the first of these roots as a function of

$$\omega_0 \equiv k_0\delta = \omega\delta/c_0$$

for various values of M.

5.2. *Factorization of the Kernel function*

Inserting (5.7) and (5.8) into (2.13) to calculate V_U and V_L and using the result in (2.31) we find that

$$K(k) = \frac{2i(kM - k_0)}{\gamma_2(k)} L_0(k), \tag{5.13}$$

where

$$L_0(k) \equiv \frac{L_N(k)}{L_D(k)} \equiv \frac{\gamma_1(k)\,(k_0 - Mk)^2 \sinh \delta\gamma_2(k) + k_0^2\,\gamma_2(k) \cosh \delta\gamma_2(k)}{\gamma_1(k)\,(k_0 - Mk)^2 \cosh \delta\gamma_2(k) + k_0^2\,\gamma_2(k) \sinh \delta\gamma_2(k)} \tag{5.14}$$

Then since $|L_0(k)| \to 1$ and $\arg L_0(k) \to 0$ as $k \to \pm\infty$, it follows that (Gakhov pp. 36 and 37; Noble pp. 15 and 16)

$$L_\pm(k) \equiv \frac{1}{2\pi i}\int_{-\infty}^{\infty} \frac{\ln L_0(k_1)}{k_1 - k}\, dk_1, \quad \operatorname{Im} k \gtrless 0 \tag{5.15}$$

are non-zero bounded analytic functions in their respective half planes of definition such that

$$L_\pm(k) = \pm \tfrac{1}{2} \ln L_0(k) + \frac{1}{2\pi i}\int_{-\infty}^{\infty} \frac{\ln L_0(k_1)}{k_1 - k}\, dk_1 \quad \text{for} \quad \operatorname{Im} k = 0, \tag{5.16}$$

where the singular integral is to be interpreted as a Cauchy principal value. Hence it follows that we can write the factorization of K implied by (2.24) as

$$K_+(k) = \frac{e^{L_+(k)}}{((1-M)k + k_0)^{\frac{1}{2}}}, \quad \operatorname{Im} k \geqslant 0, \tag{5.17}$$

$$K_-(k) = \frac{i((1+M)k - k_0)^{\frac{1}{2}}}{2(k_0 - Mk)}\, e^{L_-(k)}, \quad \operatorname{Im} k \leqslant 0. \tag{5.18}$$

The numerator and denominator, $L_N(k)$ and $L_D(k)$, of $L_0(k)$ will have a number of simple zeros that will approach the real k-axis when the small imaginary part of k_0 is just equal to zero. We denote these zeros which will always lie in the range $-k_0/(1-M) < k < -k_0$ by k_j^N, $j = 1, 2, \ldots J_N$ and k_j^D, $j = 1, 2, \ldots J_D$, respectively. Since they correspond to waves trapped in the slug flow velocity profile, which can only propagate upstream, they must approach the real axis from below. The numerator of L_0 will also have zeros at the branch points $k_0/(1+M)$, $-k_0/(1-M)$ of γ_2. These zeros will cause the imaginary part of $\ln L_0$ to change discontinuously as the real axis is traversed. In order to ensure that the appropriate branch of the logarithm is used as the integration proceeds across these zeros, it will be helpful to remove them analytically before attempting to evaluate the integrals (5.15) and (5.16). When this is done we find that

$$\frac{1}{2\pi i}\int_{-\infty}^{\infty} \frac{\ln L_0(k_1)}{k_1 - k}\, dk_1 = \tfrac{1}{4} \ln\left[\frac{(1-M)\,k + k_0}{(1+M)\,k - k_0}\right] + \tfrac{1}{2} \ln \Delta(k) + \frac{1}{i} I_1(k) + I_2(k), \tag{5.19}$$

where

$$I_1(k) = \frac{1}{2\pi}\int_{-\infty}^{\infty} \frac{\ln |L_0(k_1)|}{k_1 - k}\, dk_1, \tag{5.20}$$

$$I_2(k) = \frac{1}{2\pi}\int_{-k_0}^{k_0} \frac{\phi(k_1)}{k_1 - k}\, dk_1, \tag{5.21}$$

$$\phi(k) = \begin{cases} \arg L_0(k), & k > k_0/(1+M), \\ \arg L_0(k) + \frac{1}{2}\pi, & k < k_0/(1+M), \end{cases}$$

$$\Delta(k) = \prod_{j=1}^{J_N} \left(\frac{k-k_j^N}{k+k_0}\right) \Big/ \prod_{j=1}^{J_D} \left(\frac{k-k_j^D}{k+k_0}\right) \tag{5.22}$$

and we have omitted a possible piecewise constant imaginary additive term since the formulae of the previous section only involve the absolute values of K_+ and K_- and the imaginary part of (5.19) will therefore make no contribution. This also obviates the need to evaluate any integrals that involve both logarithmic singularities and Cauchy principal values.

5.3. *Working formulae*

Substituting (5.10) into (2.13) to calculate V_I and then inserting this together with (5.17), (5.18), and (5.19) into (2.57) we obtain

$$\mathscr{A}_F(\kappa_I, \kappa) = \left| \left(\frac{1-\kappa M}{1-\kappa_I M}\right) \left(\frac{\gamma_2(k_0\kappa_I)\,\Delta(k_0\kappa_I)}{\gamma_2(k_0\kappa)\,\Delta(k_0\kappa)}\right)^{\frac{1}{2}} \right| \frac{\exp\left[I_2(k_0\kappa_I) - \operatorname{Re} I_2(k_0\kappa) - \operatorname{Im} I_1(k_0\kappa)\right]}{|L_0(k_0\kappa_I)|^{\frac{1}{2}}} \mathscr{D}(\kappa) \tag{5.23}$$

where

$$\mathscr{D}(\kappa) = \begin{cases} 1, & \operatorname{Im}\kappa \neq 0, \\ |L_0(k_0\kappa)|^{\frac{1}{2}}, & \operatorname{Im}\kappa = 0. \end{cases}$$

Consistent with equation (2.63), we put

$$\mathscr{A}_C(\kappa_I, \kappa) = \mathscr{A}_F(\kappa_I, \kappa) \left| \frac{\kappa - \kappa_J}{\kappa_I - \kappa_J} \right|. \tag{5.24}$$

Then substituting (5.7) into (4.2) we obtain

$$|p_\lambda / p_I(0,0,0)| \sim (2\pi r k_0)^{-\frac{1}{2}} \left| \frac{\mathscr{A}_\lambda(\kappa_I, \cos\theta)\gamma_2(k_0\cos\theta)\,k_0^2}{L^N(k_0\cos\theta)\,(\kappa_I - \cos\theta)} \frac{(\kappa^* - \kappa_I)}{(\kappa^* - \cos\theta)} \right| \quad \text{as} \quad r \to \infty \quad \text{for} \quad \lambda = F, C. \tag{5.25}$$

The acoustic radiation for the case where there is no vortex shedding is given by this result with $\lambda = F$ and the factor $(\kappa^* - \kappa_I)/(\kappa^* - \cos\theta)$ put equal to one.

6. Numerical results and discussion

We have seen that there are two mechanisms that can couple the incident acoustic wave to the linear instability wave on the downstream flow. We can illustrate the principal effects of this coupling phenomena by working out numerical results for the plug flow model described in § 5. Figure 8 is a plot of the eigenvalue κ^* of the downstream instability wave. Its amplification rate is given by k_0 times the imaginary part of κ^*. The figure clearly shows that $|\operatorname{Im}\kappa^*|$ is a maximum when the Mach number is small and that for fixed M the maximum tends to occur at a Helmholtz number $\omega\delta/c_0$ (based on shear layer thickness) of about 0·27 or so. The dropoff at small values of $\omega\delta/c_0$ occurs because the plate tends to inhibit the downstream vortex shedding which is represented mathematically by the instability wave solution.

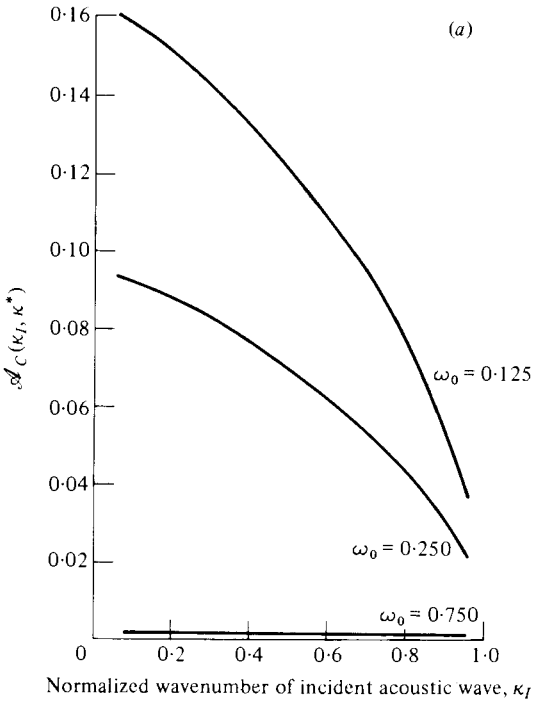

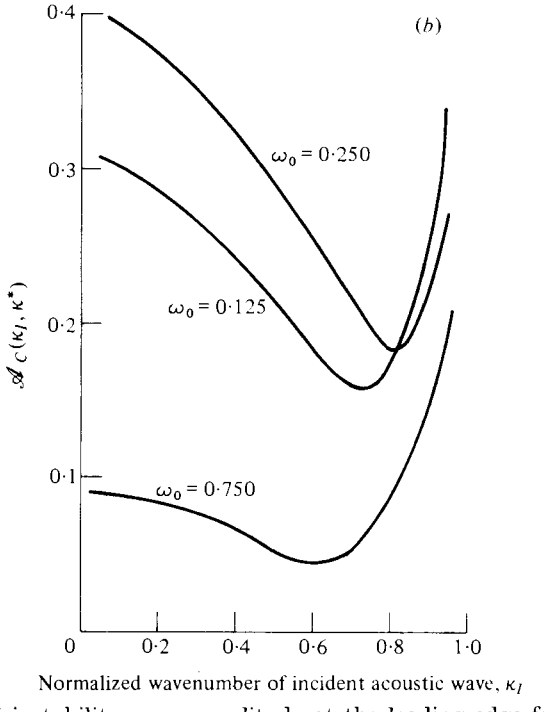

FIGURE 9. Normalized instability wave amplitude at the leading edge for the causal solution. (*a*) $M = 0{\cdot}25$, (*b*) $M = 0{\cdot}75$.

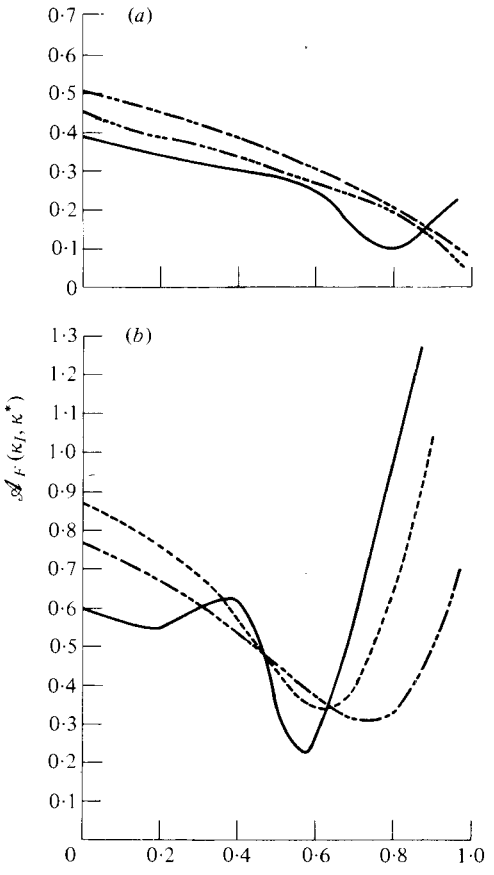

FIGURE 10. Normalized instability wave amplitude at the leading edge for the bounded solution. (*a*) $M = 0{\cdot}25$, (*b*) $M = 0{\cdot}75$. —·····—, $\omega_0 = 0{\cdot}125$; ——·——, $\omega_0 = 0{\cdot}25$; – – –, $\omega_0 = 0{\cdot}75$; ——, $\omega_0 = 3{\cdot}0$.

The amplitude of the instability waves at any point downstream of the leading edge is equal to

$$\mathscr{A}_\lambda(\kappa_I, \kappa^*)|p_I(0, 0, t)|\exp[-k_0(\mathrm{Im}\,\kappa^*)\,x],$$

where $\lambda = C$ for the causal solution and $\lambda = F$ for the solution which is non-singular at the edge. Thus $\mathscr{A}_\lambda$ represents the normalized initial (i.e. at the leading edge) amplitude of the instability wave. The instability wave will be the largest when $\mathscr{A}_\lambda$ and $\mathrm{Im}\,\kappa^*$ achieve their largest values. The initial amplification ratio $\mathscr{A}_C$ for the causal solution is plotted against κ_I, the normalized wavenumber of the incident acoustic wave, in figure 9 and the initial amplification ratio $\mathscr{A}_F$ for the bounded solution is plotted in figure 10. The results show that, unlike $\mathrm{Im}\,\kappa^*$, $\mathscr{A}_\lambda$ for $\lambda = C, F$ increases with increasing Mach number. The wavenumber κ_I is equal to the cosine of the angle that the incident wave makes with the downstream jet axis so that it is perpendicular to the plate when $\kappa_I = 0$. The figures show that $\mathscr{A}_\lambda$ generally attains its minimum for any given Mach number and Helmholtz number when the incident wave makes a certain rather small angle with the jet axis. (The minimum occurs too

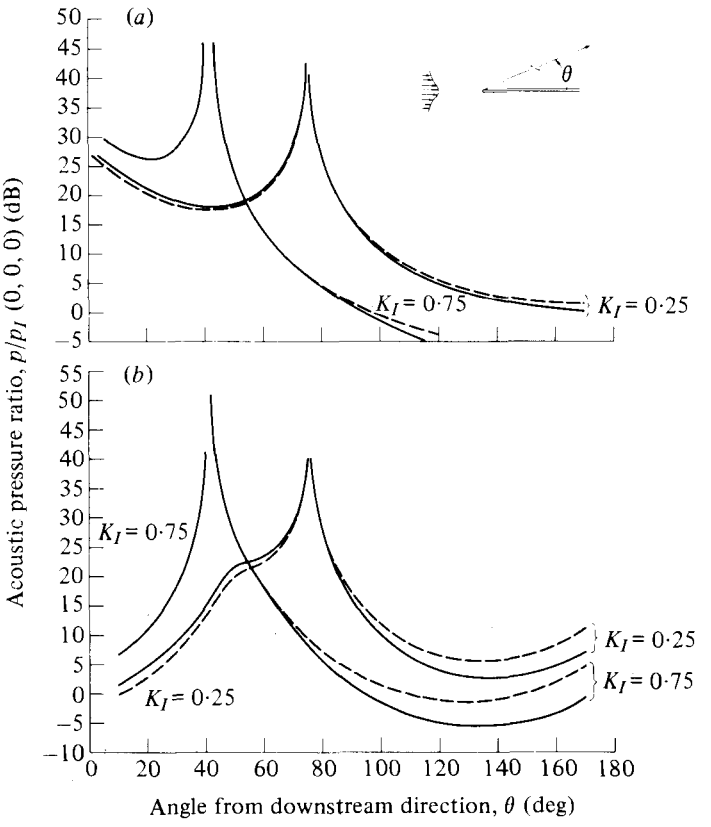

FIGURE 11. Effect of instability wave on acoustic pressure ratio. (*a*) $M = 0{\cdot}25$; $\omega_0 = 0{\cdot}25$. (*b*) $M = 0{\cdot}75$; $\omega_0 = 0{\cdot}75$. ---, causal solution; ——, solution without edge singularity.

close to $\kappa_I = 1$ to show up on figure 9(*a*).) When the incidence angle is smaller than this $\mathscr{A}_C$ tends to decrease with Helmholtz number while $\mathscr{A}_F$ tends to increase. When the incidence angle is larger than this value $\mathscr{A}_C$ reaches a maximum at a value of ω_0 near 0·125 while $\mathscr{A}_F$ reaches a maximum at a value of ω_0 that is close to value where the instability wave achieves its maximum growth rate.

We have seen that the causal solution will coincide with the solution that is bounded at infinity at frequencies above the cut-off frequency ω_J of the upstream sinuous instability. But since this cut-off frequency is infinite for the slug-flow velocity profile, it is possible that the high-frequency causal and no-vortex-shedding solutions will differ in this case. However, it is easy to see that equations (5.11) and (5.12) become equal as $\omega_0 = k_0\delta \to \infty$, which implies that $\kappa^* \to \kappa_J$ as $\omega_0 \to \infty$. Hence, it follows from (5.24) and (5.25) that the causal and bounded solutions will again have the same radiation fields in this limit.

Figure 11 is a plot of the acoustic pressure in the radiation field as a function of the angle θ measured from the downstream jet axis. The dashed curves correspond to the causal solution, and the solid curves correspond to the case where there is no vortex shedding. For the conditions shown, κ^* is so close to κ_J that there is no significant difference between the causal solution and the solution that is bounded at infinity. These two solutions will only differ when ω_0 is quite small. It can also be seen that the

solution which is non-singular at the edge is not extremely different from these two solutions; with the primary difference occurring in the upstream direction where the radiation field is small. It has frequently been suggested that the vortex shedding downstream of the edge in an edge tone experiment plays no role in the edge tone generation. The present results show that this will certainly be the case if the causal solution provides the correct coupling condition and the frequency is not too low. Otherwise there could be a small but significant effect.

The author would like to thank Dr Theodore Fessler for carrying out the numerical computations and Prof. M. V. Morkovin for his helpful comments.

Appendix A. Large-wavenumber solution to reduced wave equation

In this appendix we obtain expressions for the solution to the reduced wave equation (2.11) that satisfy the boundary conditions (2.14) and (2.15) and are valid in the limit as $k \to \infty$ while k_0 remains finite.

To this end, we first transform (2.11) into normal form by introducing the variable

$$\Pi = P/D \tag{A 1}$$

to obtain

$$\Pi'' + q\Pi = 0, \tag{A 2}$$

where D is defined in (2.12) and

$$q = D^2 - k^2 + \frac{D''}{D} - 2\left(\frac{D'}{D}\right)^2. \tag{A 3}$$

Expanding this result for large k we obtain

$$q = k^2 q_0 + k q_1 + q_2 + O(k^{-1}), \tag{A 4}$$

where

$$\left.\begin{aligned} q_0 &= -(1-M^2), \\ q_1 &= -2k_0 M, \\ q_2 &= \frac{M''}{M} - 2\left(\frac{M'}{M}\right)^2, \\ &\cdot \\ &\cdot \\ &\cdot \end{aligned}\right\} \tag{A 5}$$

Then as shown for example in Goldstein & Braun (1973) the solutions to equation (A 2) will possess an asymptotic expansion of the form

$$\Pi = e^{k\Omega(y)} \sum_{n=0}^{\infty} \tilde{p}_n(y)\, k^{-n}. \tag{A 6}$$

Inserting this along with the expansion (A 4) into (A 2) and equating coefficients of like powers of k, we obtain

$$\Omega'^2 + q_0 = 0,$$
$$\Omega''\tilde{p}_0 + 2\Omega'\tilde{p}_0' + q_1\tilde{p}_0 + (\Omega'^2 + q_0)\tilde{p}_1 = 0,$$

Hence it follows that

$$\Omega = \pm \int (1-M^2)^{\frac{1}{2}}\, dy$$

and

$$p_0 = \frac{1}{(1-M^2)^{\frac{1}{4}}} \exp\left[\pm k_0 \int \frac{M}{(1-M^2)^{\frac{1}{2}}}\, dy\right].$$

Then corresponding to these two signs, (A 2) will possess the two linearly independent asymptotic solutions

$$\Pi_\pm = \frac{\exp[\pm \int [k(1-M^2)^{\frac{1}{2}} + k_0 M(1-M^2)^{-\frac{1}{2}}]\, dy]}{(1-M^2)^{\frac{1}{4}}} + O(k^{-1}). \tag{A 7}$$

Since

$$(k^2-(k_0-Mk)^2)^{\frac{1}{2}} \equiv \gamma(k,y) = \pm[k(1-M^2)^{\frac{1}{2}} + k_0 M(1-M^2)^{-\frac{1}{2}}] + O(k^{-1}), \quad k \gtrless 0, \tag{A 8}$$

when we choose the branch of the square root in the manner indicated in figure 6, it follows from (A 1) that the asymptotic solutions to (2.11) that correspond to P_U, P_L and therefore satisfy the boundary conditions (2.14) and (2.15) with the choice of branch shown in figure 3, can be written as

$$P_{U/L} = \frac{D\, e^{\mp \int \gamma(k,y)dy}}{(1-M^2)^{\frac{1}{4}}} + O(k^{-1}) \quad \text{for} \quad y \gtrless 0 \quad \text{as} \quad k \to \infty. \tag{A 9}$$

Appendix B. Asymptotic behaviour of the factors of the Kernel function

In this appendix we use the asymptotic solutions of appendix A to determine the behaviour of $K_\pm$ as $k \to \infty$.

Inserting (A 9) into (2.13) we find that

$$V_{U/L} = \frac{\pm\gamma}{iD} P_{U/L} \quad \text{for} \quad y \gtrless 0 \quad \text{as} \quad k \to \infty.$$

Hence it follows from (2.12), (2.19), and (2.24) that

$$K_+(k)/K_-(k) = K(k) = \frac{2i(kM-k_0)}{\gamma} K_0, \quad \operatorname{Im} k = 0, \tag{B 1}$$

where

$$|K_0| \to 1$$

and

$$\arg K_0 \to 0 \quad \text{as} \quad k \to \pm\infty.$$

It therefore follows (Noble 1958, pp. 15 and 16, note equation (1.21)) that we can factor K_0 into the ratio $K_0 = K_0^+/K_0^-$ of two functions $K_0^\pm$ that are analytic in the upper/lower half plane such that K_0^+ is bounded and non-zero as $k \to \infty$ in the upper half plane and K_0^- is bounded and non-zero as $k \to \infty$ in the lower half plane. We

therefore conclude from (A 8), (B 1), figure 6, and the fact that k_0 has a small positive imaginary part that

$$K_+ \sim \frac{1}{(k+k_0/(1-M))^{\frac{1}{2}}} \sim k^{-\frac{1}{2}} \quad \text{as } k \to \infty \text{ in the upper half plane,} \tag{B 2}$$

$$K_- \sim \frac{(k-k_0/(1+M))^{\frac{1}{2}}}{kM-k_0} \sim k^{-\frac{1}{2}} \quad \text{as } k \to \infty \text{ as in the lower half plane.} \tag{B 3}$$

REFERENCES

Bechert, D. & Pfizenmaier, E. 1975 *J. Fluid Mech.* **71**, 123–144.

Betchov, R. & Criminale, W. O. 1967 *Stability of Parallel Flows*. Academic.

Bratt, J. B. 1953 Flow patterns in the wake of an oscillating airfoil. *Aero. Res. Counc. R & M* 2773.

Briggs, R. J. 1964 Electron stream interactions with plasmas. Massachusetts Institute of Technology Press.

Brown, S. N. & Daniels, P. G. 1975 *J. Fluid Mech.* **67**, 743–761.

Crighton, D. G. & Leppington, F. G. 1974 *J. Fluid Mech.* **64**, 393–414.

Daniels, P. G. 1978 *Quart. J. Mech. Appl. Math.* **31**, 49–75.

Drazin, P. G. & Howard, L. M. 1966 Hydrodynamic stability of parallel flow of inviscid fluid. In *Advances in Applied Mechanics*, vol. 9, pp. 1–90. Academic.

Gakhov, F. D. 1966 *Boundary Value Problems*. Addison-Wesley.

Goldstein, M. E. 1976 *Aeroacoustics*. McGraw-Hill.

Goldstein, M. E. 1978 *J. Fluid Mech.* **84**, 305–329.

Goldstein, M. E. 1979 *J. Fluid Mech.* **91**, 601–632.

Goldstein, M. E. & Braun, W. H. 1973 Advanced methods for the solution of differential equations. *N.A.S.A.* SP-316.

Gottlieb, P. 1959 Acoustics in moving media. Ph.D. thesis, Massachusetts Institute of Technology.

Hardisty, M. 1974 The effect of sound on vortex sheets. Ph.D. thesis, University of Dundee.

Heavens, S. N. 1978 *J. Fluid Mech.* **84**, 331–335.

Kovasznay, L. S. G. & Fujita, H. 1973 *Recent Research on Unsteady Boundary Layers, Proc. IUTAM Symp.* 1971, vol. 1, pp. 806–833. Presses de l'Universite Laval.

Morkovin, M. V. 1969 *Air Force Flight Dyn. Liab. Rep.* AFFDL-TR-68-149.

McCartney, M. S. & Grebe, I. 1973 An experimental and theoretical investigation of edgetone phenomenon. *Dept. Fluid, Thermal & Aerospace Sci., Case Western Reserve Univ.* FTAS TR-73-87.

Noble, B. 1958 *Methods Based on the Wiener–Hopf Technique for the Solution of Partial Differential Equations*. Pergamon.

Ohashi, H. & Ishikawa, N. 1972 *Bull. J.S.M.E.* **15** (85), 840–847.

Rienstra, S. W. 1979 Edge influence on the response of shear layers to acoustic forcing. Doctor in de Technische Wetenschappen Dissertation, Technische Hogeschool, Eindhoven.

Roos, B. W. 1969 *Analytic Functions and Distributions in Physics and Engineering*. Wiley.

Tam, C. K. W. 1971 *J. Fluid Mech.* **46**, 757–768.

Wagner, H. 1925 *Z. angew. Mach. Mech.* **5**, 17–35.